Undrained capacity of circular shallow foundations under combined VHMT loading

Pengpeng HE[a] and Tim NEWSON[a,1]
[a] *Geotechnical Research Centre, Department of Civil & Environmental Engineering, Western University, Canada*

Abstract. Torsional loads can be significant on shallow foundations for large onshore structures, such as wind turbines. However, torsional effects for circular foundations under a zero-tension interface condition have not been well studied. This paper shows the results of finite element analysis of circular foundations with a no-tension interface under combined vertical, horizontal, moment and torsional loading. Similar equations to current forms of *V-H* expression are applied to model the *V-T* relationship. The normalized *H-T* and *M-T* envelopes have been simulated with existing analytical equations, but with some modifications. The developed approaches will provide improved design methods for estimating torsional capacity of shallow foundations.

Keywords. Circular foundation, no-tension interface, failure envelope, torsional load, finite element analysis.

1. Introduction

Shallow foundations have been extensively used to support large onshore structures, such as wind turbines, transmission towers and masts. Load-bearing capacity of shallow foundations under combined loading is of great significance, since foundations are generally subjected to various load combinations due to environmental loads. Typical analytical methods for this type of design are based on classical solutions for the uniaxial vertical bearing capacity of shallow foundations. To account for the effect of load inclination and eccentricity, the load inclination factor and the effective foundation area are introduced in the conventional method, as recommended by some geotechnical design guidelines (e.g. DNVGL-ST-0126 [1], API [2]). However, this simple, traditional method may not be accurate enough in practical design because the load inclination and eccentricity effects are separately considered [3].

Another choice for foundation design under combined loads is the failure envelope method, which can explicitly incorporate the load interaction effect between various load components [4]. This method has been recommended as an alternative to conventional theory in API [2] and ISO [5]. Failure envelopes for different types of foundations (e.g. strip [6], rectangular [7] and circular [8] foundations), homogeneous [9] or non-homogeneous [10] soils, and zero-tension [8] or unlimited-tension [7] interface

[1] Corresponding Author: Tim NEWSON, Geotechnical Research Centre, Department of Civil & Environmental Engineering, Western University, Canada; Email: tnewson@eng.uwo.ca.

conditions have been investigated. These studies on the failure envelope method have been mainly confined to load combinations of vertical, horizontal and moment loads. However, environmental loads on the structure are often not co-planar and transverse loads can also induce torsional effects to the foundation [11]. Thus, torsional loads should also be considered for the failure envelope of shallow foundations.

The object of this paper is to investigate the VHMT failure envelope of circular surface foundations under a zero-tension interface condition for undrained soils using finite element analysis.

2. Finite element analysis

2.1. Geometry and mesh

The finite element (FE) analysis in this paper was conducted using the software ABAQUS [12]. This study has considered circular foundations resting on the free surface of the soil. The size of the foundation was chosen to represent typical dimensions for wind turbines used in Canada. The foundation has a diameter of D=19 m and a thickness of t=3 m. To avoid the effects of model boundaries on the development of failure mechanisms, the mesh length L and mesh height h are taken as 120 m and 50 m, following the recommendations of Deshpande [13].A mesh convergence study was also carried out using three mesh densities, as shown in Figure 1(a). It shows that Mesh 2 with about 39000 8-noded brick elements (see Figure 1(b)) is a reasonable choice.

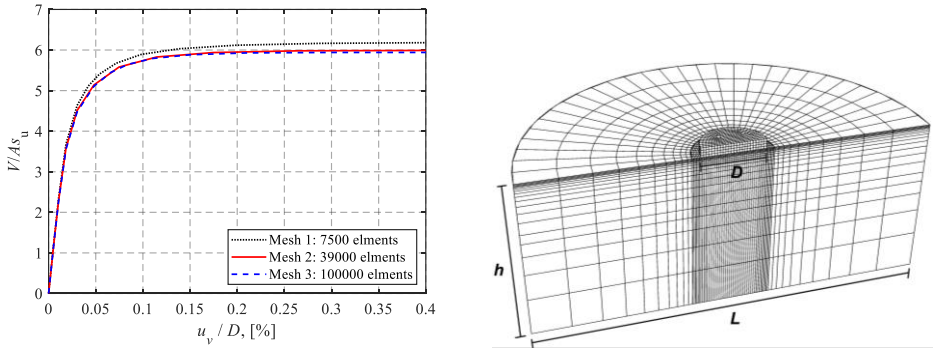

(a) Mesh convergence study (b) Half-view of the FE mesh (Mesh 2)

Figure 1. Mesh convergence study and half-view of the FE mesh

To capture the intense stress concentration close to the foundation edge and the large plastic shear strains at the interface, the soil regions in the vicinity of the foundation edge and the horizontal thin soil layer close to the interface were carefully refined.

2.2. Material models and interface conditions

A linear elastic perfectly plastic constitutive relationship with a Mohr-Coulomb (M-C) failure criterion was used to model the soil behavior. For undrained conditions, the M-C criterion degenerates to the Tresca criterion, which is defined by 3 soil parameters: the undrained Young's modulus, E_u, Poisson's ratio, μ, and the undrained shear strength, s_u.

To account for the soil strength heterogeneity, the undrained soil shear strength was considered to linearly increase with depth from the ground (see Figure 2):

$$s_{\mathrm{u}} = s_{\mathrm{u0}} + kz \tag{1}$$

where s_{u0} is the undrained shear strength at foundation level; k is the strength increase per depth. s_{u0} is taken as 100 kPa. The dimensionless soil strength heterogeneity ratio defined by $\kappa = kD/s_{\mathrm{u0}}$ [7] was taken as 0 (homogeneous soil), 2, 6 and 10. The Poisson's ratio of the undrained soil was taken as 0.49. In the present study, a sufficiently large $E_{\mathrm{u}}/s_{\mathrm{u0}}$ ratio of 10000 was selected to minimize mesh distortion (Abyaneh et al. [14]). The foundation was assumed to be a rigid body. A load reference point (LRP), which was used to apply prescribed displacements or loads, was attached to the bottom center of the foundation, as shown in Figure 2.

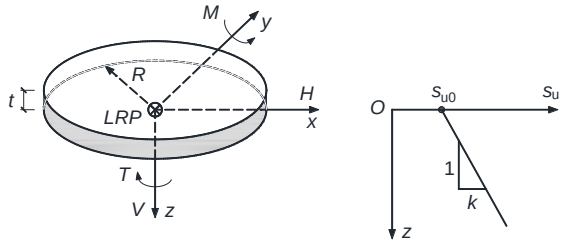

Figure 2. Sign conventions and soil strength profile

Similar to Shen et al. [8], the FE analysis considered a no-tension interface that allows separation of the foundation from the soil. As demonstrated by Shen et al. [8], the friction coefficient of the Coulomb friction can be assumed to be 20°.

2.3. Sign conventions and loading paths

The sign conventions for the loads are shown in Figure 2. In the analysis, the horizontal and moment loads were considered to be in the same plane.

Probe tests and swipe tests were employed to detect the failure envelopes under various load conditions. In a probe analysis, a vertical load is first applied at the LRP of the foundation and remains constant. A fixed-ratio of displacement is then imposed to the foundation to track the failure point on the failure envelope.

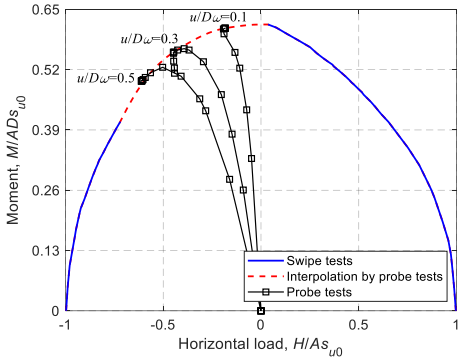

Figure 3. *M-H* failure envelope for κ=0 at V / V_{ult} = 0.50

The swipe test, which was introduced by Tan [15], brings the foundation to a collapse state in coordinate direction 1 first (displacement-controlled), followed by a displacement applied in coordinate direction 2, during which the increment of the displacement in coordinate direction 1 remains zero (Gourvenec and Randolph by [7]). For some cases the swipe test cannot capture the entire failure envelope due to convergence issues, hence a probe test is carried out to facilitate the analysis. An example obtained using a combination of swipe and probe tests is shown in Figure 3.

3. Finite element results

3.1. Pure uniaxial capacity

The ultimate loads for vertical, horizontal and torsional modes are referred to as the corresponding uniaxial load-carrying capacities without other loading modes. As the foundation with a no-tension interface cannot resist moment loading if no vertical load is prescribed, the ultimate moment capacity is represented by the maximum moment load only under vertical loading [8]. The uniaxial bearing capacity factors are defined as:

$$\begin{aligned} v_0 &= V_{\mathrm{ult}}/(As_{\mathrm{u0}}); \quad & h_0 &= H_{\mathrm{ult}}/(As_{\mathrm{u0}}) \\ m_0 &= M_{\mathrm{ult}}/(ADs_{\mathrm{u0}}); \quad & t_0 &= T_{\mathrm{ult}}/(ADs_{\mathrm{u0}}) \end{aligned} \tag{2}$$

where A is the soil-foundation contact area.

The FE-calculated v_0, h_0, m_0 and t_0 for soils with different heterogeneity ratios are compared in Table 1 with other reported values from the literature.

Table 1. Uniaxial bearing capacity factors for soils with different heterogeneity ratios

κ	0	2	6	10	0	2	6	10
	v_0				h_0			
This study	6.00	7.51	9.59	11.29	1.00	1.00	0.99	1.00
Shen et al. (2016)	5.87	7.42	9.56	11.28	1.02	1.02	1.03	1.03
	m_0				t_0			
This study	0.62	0.74	0.91	1.03	0.33	0.33	0.33	0.34
Shen et al. (2016)	0.61	0.72	0.89	1.03	--	--	--	--

The comparison shows close agreement of v_0, h_0 and m_0 (difference less than 3%) between this study and the results of Shen et al. [8]. Similar to the horizontal bearing capacity, the torsional bearing capacity exhibits independence from the heterogeneity ratio as the failure state for horizontal and torsional modes is only reached when the shear stress of s_{u0} is fully developed.

3.2. Vertical-Torsion, Horizontal-Torsion and Moment-Torsion loading

For brevity, since the main objective of this analysis is to study the effect of torsional loading on the failure envelope of the foundation, only the vertical-torsion, horizontal-torsion and moment-torsion failure envelopes are discussed in this section.

3.2.1. Vertical-Torsion loading

The *V-T* failure envelopes for soils with different soil heterogeneity ratios are shown in Figure 4. As shown in Figure 4(b), the *V-T* envelopes normalized by the corresponding ultimate capacities collapse into a narrow band regardless of the heterogeneity ratios.

Feng et al. [10] provided an expression for the normalized *V-T* failure envelopes for rectangular foundations with an unlimited-tension interface, which was then used by Shen et al. [4] to apply to a zero-tension interface:

$$T/T_{\text{ult}} = [1 - 4(V/V_{\text{ult}} - 0.5)^2]^{0.4}, \text{ for } V/V_{\text{ult}} > 0.5 \quad (3a)$$

$$T/T_{\text{ult}} = 1, \text{ for } V/V_{\text{ult}} \leq 0.5 \quad (3b)$$

Abyaneh et al. [14] proposed a similar equation for circular foundations under an unlimited-tension interface condition:

$$V/V_{\text{ult}} = 0.5 + 0.5[1 - (T/T_{\text{ult}})^{2.5}]^{0.3}, \text{ for } V/V_{\text{ult}} > 0.5 \quad (4a)$$

$$T/T_{\text{ult}} = 1, \text{ for } V/V_{\text{ult}} \leq 0.5 \quad (4b)$$

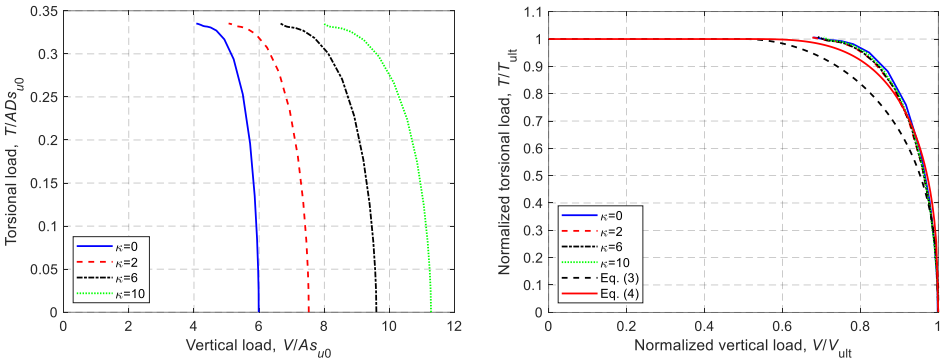

(a) Dimensionless *T-V* (b) Normalized *T-V*

Figure 4. Dimensionless and normalized *T-V* failure envelopes

Eqs. (3) and (4) are also presented in Figure 4 for comparison. This shows that Eq. (4) can provide a reasonable approximation, although it was developed for an unlimited-tension interface. In contrast, Eq. (3) gives more conservative results compared with the FE-calculated curves.

3.2.2. Horizontal-Torsion-Vertical loading

Figure 5 presents the normalized *H-T* failure envelopes for V / V_{ult} = 0.50. Finnie and Morgan [16] proposed Eq. (5) to model the *H-T* relationship without moment:

$$(H/H_{\max})^l + (T/T_{\max})^n = 1 \tag{5}$$

where $H_{\max}$ and $T_{\max}$ are the maximum horizontal and torsional loads for a given V/V_{ult}.

As shown before, for $V/V_{\text{ult}} \leq 0.5$, $H_{\max} = H_{\text{ult}}$ and $T_{\max} = T_{\text{ult}}$ (see Eq. (3b)). For $V/V_{\text{ult}} > 0.5$, $T_{\max}$ at $V/V_{\text{ult}} > 0.5$ can be calculated from Eq. (3a) as:

$$T_{\max} = [1 - (2\,V/V_{\text{ult}} - 1)^{3.33}]^{0.4} \cdot T_{\text{ult}} \tag{6}$$

$H_{\max}$ for $V/V_{\text{ult}} > 0.5$ can be evaluated using Green's original solution [17] as $H_{\max} = [1 - (2\,V/V_{\text{ult}} - 1)^2] \cdot H_{\text{ult}}$

The dimensionless powers, l and n in Eq. (5), depend on foundation geometry. Feng et al. [10] proposed Eq. (7) to estimate l and n based on the FE analysis of rectangular foundations with the unlimited-tension interface:

$$l = 1.85;\ n = 1.25 + 0.75(\sin\theta)^{2.5} \tag{7}$$

where θ is the loading direction for rectangular foundations. Yun et al. [18] recommended $l = n = 1.75$ for circular and square foundations.

The curves of Eq. (5) for $\theta = 0, 90^{\circ}$ in Eq. (7) and $l = n = 1.75$ are also presented together with the FE-calculated results in Figure 5. For the case of $V / V_{\text{ult}} = 0.50$, $l = n = 1.75$ can be considered to be a better choice to fit the *H-T* failure envelopes.

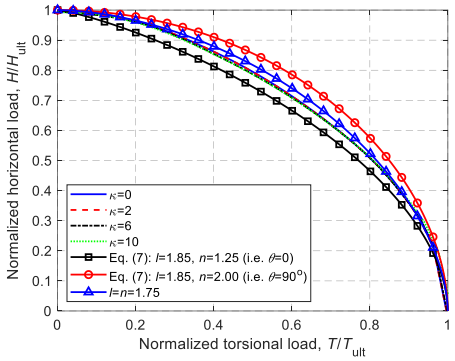

Figure 5. *H-T* failure envelopes at $V / V_{\text{ult}} = 0.50$

3.2.3. Moment-Torsion-Vertical loading

The ultimate load-carrying capacity under moment and torsional loading at $V / V_{\text{ult}} = 0.50$ for the four soil heterogeneity ratios is compared in Figure 6. As shown in Figure 6, the *M-T* failure envelopes normalized by the corresponding ultimate loads fall within narrow bands, which eliminates their dependence on the soil heterogeneity ratio.

Shen et al. [4] proposed a *M-T* relationship for rectangular foundations under a zero-tension interface condition:

$$(M/M_{\max})^{\alpha} + (T/T_{\max})^{\beta} = 1, \text{ for } V/V_{\text{ult}} \leq 0.5 \text{ and } 0 \leq \kappa \leq 10 \tag{8}$$

where α and β are dimensionless parameters. Shen et al. [4] suggested $\alpha = 1.5$ and $\beta = 2.0$. Based on the results of rectangular foundations with an unlimited-tension interface, Feng et al. [10] obtained two different powers: $\alpha = 6.0$ and $\beta = 2.0$.

The calculation of $T_{\max}$ also follows Eq. (6). $M_{\max}$ for different vertical load mobilizations can be evaluated based on the relationship between M and V proposed by Gourvenec [3]:

$$M/M_{\text{ult}} = 4\left[V/V_{\text{ult}} - (V/V_{\text{ult}})^2\right] \tag{9}$$

The comparison between these two relationships and this study is also shown in Figure 6. It can be seen that the curves produced with $\alpha = 1.5$ and $\beta = 2.0$ always lie inside the true failure envelopes, while the case of $\alpha = 6.0$ and $\beta = 2.0$ predicts envelopes that go significantly beyond the FE-calculated results. To gain better predictions of the current study, α and β of Eq. (8) can be adjusted. As shown in Figure 6, the case of $\alpha = 2.5$ and $\beta = 2.0$ can provide more satisfactory predictions.

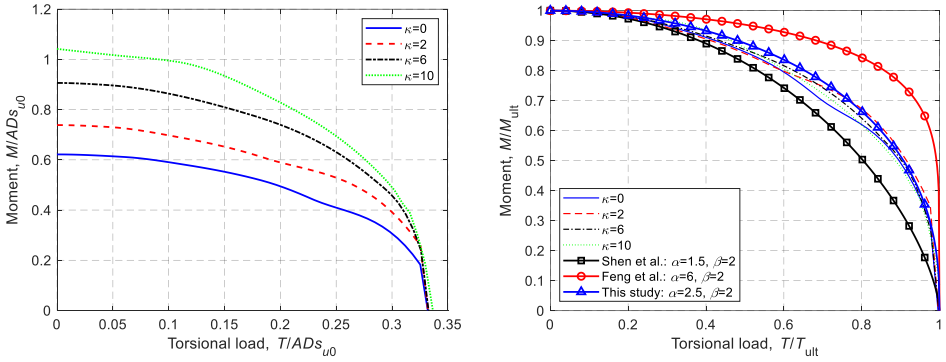

(a) Dimensionless *M-T* at $V / V_{\text{ult}} = 0.50$ (b) Normalized *M-T* at $V / V_{\text{ult}} = 0.50$

Figure 6. *M-T* failure envelopes at $V / V_{\text{ult}} = 0.50$: (a) Dimensionless *M-T* and (b) Normalized *M-T*

4. Conclusions

V-T and *H-T* and *M-T* failure envelopes of a circular surface foundation under a zero-tension interface condition have been studied using finite element analysis. Four soil strength heterogeneity ratios were considered. The *V-T* envelopes can be simulated by equations similar to current forms of *V-H* expression. The analytical equations proposed by previous researchers can also provide reasonable predictions for current *H-T* and *M-T* envelopes, but different power coefficients should be used. These approaches should aid the assessment of the torsional capacity of shallow circular foundations under complex loading conditions.

Acknowledgements

The writers would like to acknowledge the financial support of Natural Sciences and Engineering Research Council. The first author is grateful for the financial support of the China Scholarship Council (CSC).

References

[1] DNV, GL, DNVGL-ST-0126 (2006). Design of support structures for offshore wind turbines.

[2] API (2011). Recommended Practice for Geotechnical Foundation Design Consideration.

[3] Gourvenec, S. (2007). Shape effects on the capacity of rectangular footings under general loading. Géotechnique, 57(8), 637-646.

[4] Shen, Z., Feng, X., & Gourvenec, S. (2017). Effect of interface condition on the undrained capacity of subsea mudmats under six-degree-of-freedom loading. Géotechnique, 67(4), 338-349.

[5] ISO. (2016). Petroleum and natural gas industries–Specific requirements for offshore structures–Part 4: Geotechnical and foundation design considerations (2nd Edition).

[6] Bransby, M. F., & Randolph, M. F. (1998). Combined loading of skirted foundations. Géotechnique, 48(5), 637-655.

[7] Gourvenec, S., & Randolph, M. (2003). Effect of strength non-homogeneity on the shape of failure envelopes for combined loading of strip and circular foundations on clay. Géotechnique, 53(6), 575-586.

[8] Shen, Z., Feng, X., & Gourvenec, S. (2016). Undrained capacity of surface foundations with zero-tension interface under planar VHM loading. Computers and Geotechnics, 73, 47-57.

[9] Taiebat, H. A., & Carter, J. P. (2010). A failure surface for circular footings on cohesive soils. Géotechnique, 60(4), 265-273.

[10] Feng, X., Randolph, M. F., Gourvenec, S., & Wallerand, R. (2014). Design approach for rectangular mudmats under fully three-dimensional loading. Géotechnique, 64(1), 51-63.

[11] Bienen, B., Gaudin, C., & Cassidy, M. J. (2007). Centrifuge tests of shallow footing behaviour on sand under combined vertical-torsional loading. International Journal of Physical Modelling in Geotechnics, 7(2), 01-21.

[12] Dassault Systèmes (2016). Abaqus analysis user's manual. Simulia Corp, Providence, RI, USA.

[13] Deshpande, V. M. (2016). Numerical Modelling of Wind Turbine Foundations subjected to Combined Loading. Master's thesis, The University of Western Ontario.

[14] Abyaneh, S. D., Ojo, A., Maconochie, A., & Haghighi, A. (2015). The undrained bearing capacity of shallow foundations subjected to three-dimensional loading including torsion. In The 25th International Ocean and Polar Engineering Conference. International Society of Offshore and Polar Engineers.

[15] Tan, F. S. C. (1990). Centrifuge and theoretical modelling of conical footings on sand. Ph.D. thesis, Cambridge University.

[16] Finnie, I. M. S., & Morgan, N. (2004). Torsional loading of subsea structures. In The 14th International Offshore and Polar Engineering Conference. International Society of Offshore and Polar Engineers.

[17] Green, A. P. (1954). The plastic yielding of metal junctions due to combined shear and pressure. Journal of the Mechanics and Physics of Solids, 2(3), 197-211.

[18] Yun, G. J., Maconochie, A., Oliphant, J., & Bransby, F. (2009). Undrained capacity of surface footings subjected to combined VHT loading. In The 19th International Offshore and Polar Engineering Conference. International Society of Offshore and Polar Engineers.